

## Authenticity of pore size distributions obtained by traditional techniques

Dmitrii K. Efremov and Vladimir B. Fencelonov

Institute of Catalysis, prospect akademika Lavrentieva 5, Novosibirsk 630090, Russia.

**Abstract** - This work is devoted to the authenticity examination of pore size distributions which are result of some conventional interpretation techniques for independent pores. The present investigation is based on computer experiments simulating adsorption, capillary condensation, desorption, mercury intrusion and some other processes in model porous lattice made up of a large number of spheroidal-shaped voids pasted together by toroidal-shaped necks. Special attention has been paid to plausibility of simulating processes. In particular, the cooperative capillary condensation inside the group of neighbouring voids has been analyzed in terms of thermodynamics and molecular physics. The results of long-duration numerical experiments ( adsorption isotherms, mercury intrusion curves, etc.) have been processed with the help of conventional techniques calculating independent pore size distributions. Size distributions obtained this way have been compared with those generated for corresponding model porous solids, the reasons of mismatches have been also analyzed. Conclusions concerning with more reliable interpretation of results obtained by traditional techniques have been made.

### INTRODUCTION

To solve numerous problems, which arise from preparation, development and investigation of catalysts, supports and adsorbents the information on the pore volume and surface area and corresponding pore size distributions (PSD) is needed. Usually, the standard adsorption-capillary and mercury porosimetry techniques are used to get such information. However, obtaining of end-point quantitative characteristics by these techniques is based on excessively simplified model visualizing of porous space as the group of independent pores exhibiting the simplest geometric configuration (e.g., cylinders, slit shape pores, practically closed spherical voids, or cavities between regularly packed spherical particles). Such simplifications neglecting the spatial connection between elements of model porous space cause the distortion of quantitative ratios describing the model capillary condensation, desorption, mercury penetration, etc. in hole porous space. The role of this problem becomes more evident when one looks at the plot of Dullien et al. (ref. 1) (see Fig.1 in this paper), which was published later in the well known book by Greg and Sing (ref. 2). This figure shows the frequency (density) function of volume pore size distribution of one and the same porous

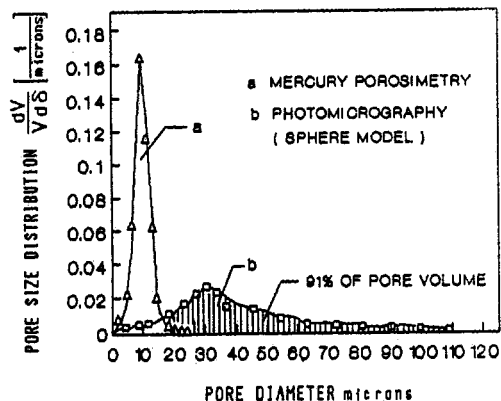


Fig. 1. Figure 9 from ref. 1.

solid. The left sharp narrow peak results from usual quantitative processing of mercury penetration curve. The other curve was produced from photomicrography of porous solid cross-section by methods of quantitative stereology applied to so-called sphere pore segment (SPS) model.

The authors of refs. 1 and 2 have tried to explain such a sharp distinction between position and form of distributions by assumption that material under consideration has a substantial difference between sizes of voids and constrictions (necks) in the pore space: the former influence in the main microscope data, the latter - mercury porosimetry ones, so far as the necks retard the advance of menisci into the porous sample. The explanation of this distinction supplied in refs. 1 and 2 do not cover all the reasons having caused such a strong effect and do not answer the question: how far is each of the distribution discussed from reality?

In the presented work, the problem under consideration have been analyzed as applied to PSDs, which have been calculated from nitrogen adsorption and desorption isotherms, mercury penetration curve and random chord length distribution obtained during corresponding computer experiments for one and the same model porous solid.

## BRIEF REVIEW OF THE PROBLEM

At the present moment one can cast doubt on most of theoretical suggestions forming the basis of quantitative estimation of PSD. For example, several years ago a number of works was published (refs. 3 - 10) where conclusion of De Boer et al. (ref. 11) that Kelvin equation is a too rough approximation (for estimation of critical relative vapor pressure at which mesopore spontaneous filling occurs) was confirmed. Moreover, density of layer adsorbed on the pore wall as well as condensate density after capillary filling considerably increase with enhancement of the relative vapor pressure,  $P/P_s$ , in the system. The last factor is not taken into consideration in conventional calculation techniques either, though recently the approach was published accounting for the above-mentioned factors in terms of the local density functional theory (ref. 10).

Much more grave disadvantage of conventional methods of PSD calculation is, in our view, spatial separation (disconnection) of model capillaries. It is shown in refs. 12 and 13 in terms of percolation theory (ref. 14) how strongly it can influence the desorption interpretation. Despite the fact that the percolation methods of calculating the neck radius distribution are based on the known void size distribution calculated without regard for their spatial connection (at the capillary condensation) the suggested in ref. 13 approach can provide, in our opinion, a more realistic estimation of mesoporous materials characteristics than the independent pore model.

Finally, both the widely spread and the most complicated methods of quantitative estimation of PSD (refs. 10, 11, 15 and 16) do not take into consideration influence of the so-called cooperative filling of neighboring pores whose possibility was foretold long ago, e.g. (ref. 17). We have sufficient grounds to suppose that in the space of pore networks the above phenomenon can have a determining effect on the adsorption branch of isotherms and, hence, introduce more serious distortions in position and form of PSDs, calculated by conventional methods. To justify this viewpoint we have performed a thoroughly planned and theoretically substantiated numerical experiments simulating adsorption and desorption measurements in model system of interrelated cavities with exactly determined individual and "collective" geometrical characteristics. Additionally, the experiments on mercury intrusion and those on random chord length distribution were carried out in the same model porous solid for which the adsorption-capillary processes were studied. The obtained model isotherms, porogram and chord length distribution were processed by conventional methods and calculated PSDs were compared with the given (predetermined) radius distributions.

## MODEL POROUS SPACE

The model porous space used presents to some extent the analog of the known model of intersecting spheres. Fig. 2 shows the section of separate void with two necks. The sharp ring-like protrusions in the place of spheres intersection are smoothed by toroidal-shaped surfaces of the same radius,  $\rho_0$ , (0.5 nm). Horizontal cross-hatching designates the pseudo-liquid phase and double cross-hatching identifies the solid one. As can be easily seen from the figure all elements of liquid-vapor configuration are uniquely determined by radii of the forming sphere,  $r_p$ , and those of necks ( $r_1, r_2$ ), by the thickness of adsorption film,  $t$ , radius of meniscus,  $R_k$ , and that of near-neck toroidal chamfers,  $\rho_0$  (see Appendix for details). Similarly, all configurations of indented mercury are uniquely determined on the basis of geometric sizes, the values of meniscus radius and contact angle between mercury and solid surface.

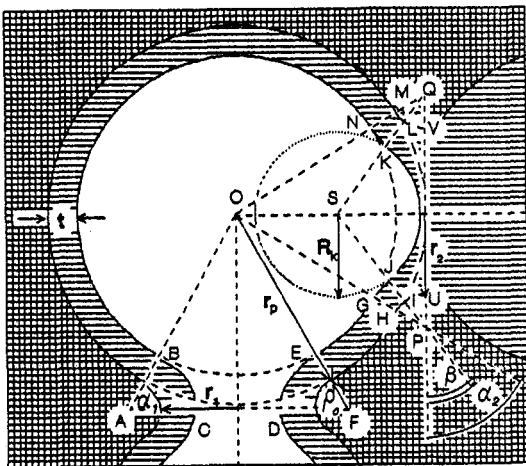


Fig. 2. Model scheme of adsorption development in interrelated voids.

To illustrate our conclusions more emphatically we shall restrict ourselves to the case when all the voids have the same radius of the forming sphere (5 nm). Computer memory saved permanently only neck radii generated previously using the random number generator so that radii values were distributed at the size interval of 1.4 - 4.2 nm with certain predetermined density (first histogram at the left, Fig. 6). The relative position of porous space elements was uniquely determined by the system of addresses in the memory (ref. 18). Thus, at any vapor pressure one could restore (orienting at the thickness of multimolecular layer and the known radii of menisci and near-neck chamfers) all the liquid-vapor configurations in any concrete void and in all the nearest and more distant neighbouring cavities. This allowed to perform the successive cyclic analysis of the possibility of cooperative filling of neighbouring cavities groups basing on thermodynamic approach formulated below (corrected on the basis of particular results of molecular physics (refs. 3 - 10). Similarly, at mercury intrusion or vapor desorption one could calculate all the volumes of mercury or pseudo-liquid inside any of the cavities.

For simplicity, all the voids had 6 (non-intersecting) necks located at an angle of  $90^\circ$  to each other. At the same time it means that the model porous space had the topology of a simple cubic lattice. Finally, to better illustrate the influence of cooperative effects we have tried to choose the model lattice made up of sufficiently large number of voids ( $\approx 3 \cdot 10^5$ ).

The described model porous space is on the one hand, simple enough for mathematical description of appearing mercury, liquid etc. configurations, and on the other hand it is rather flexible for investigating the influence of average integral curvature of surface on the processes studied. In fact, increasing the radius of neck toroidal chamfers one can perform the transfer from typically spongy porous space to the structure close in a number of properties to corpuscle structures.

### SOME ASPECTS OF THEORY OF COOPERATIVE FILLING OF VOIDS

Up to now filling of voids the scientists were able to approximately calculate the relative adsorptive pressure at which the irreversible capillary condensation occurs for the simplest geometrical shapes only. Recently, Efremov and Felonov (ref. 19) have proposed a general equation in terms of the surface shape factor and formal thickness of adsorption layer. The scope of a more accurate equation with due regard for attractive pore wall potential basing on Broekhoff and De Boer (ref. 11) or Nicholson (ref. 16) approach has been considered there too. These formal mathematics manipulations are not convenient for realization in any concrete geometry. They were meant for illustration of some ideas associated with presence of necks and possibility of cooperative spontaneous filling of neighbouring voids groups. Below we present some derivations in more suitable geometric terms, obtain the relationship of Kelvin type and then show how one can correct it for the influence of pore walls and intermolecular interaction between the pseudoliquid films on the "opposite" pore walls. As many others (refs. 20 - 22) we shall begin with reference to a well known Gibbs work (ref. 23) and consider the change in free energy,  $dG$ , in the pore (cavity) upon condensation of  $dN$  moles of substance from the gas phase to the "adsorbed layer" at constant temperature,  $T$ , and pressure,  $P$ :

$$dG_{P,T} = (\mu_L - \mu_g) \cdot dN + \gamma \cdot dA \quad (1)$$

where  $dA$  is the change of interface area;  $\mu_L$  and  $\mu_g$  are the chemical potentials of liquid and vapor,  $\gamma$  is interfacial tension. Dividing both the parts of equation (1) by  $dN$ , supposing the adsorptive to possess the properties of an ideal gas ( $\mu_L - \mu_g = RT \ln(P_s/P)$ ) and noting that at equilibrium  $dG = 0$ , we can write this expression in a following way:

$$RT \ln(P_s/P) = -\gamma \cdot dA/dN \quad (2)$$

Assuming the molar volume of pseudoliquid adsorbed substance,  $v_m$ , is constantly equal to the similar value for the bulk liquid ( $dV = dN/v_m$ ) we obtain from (1) and (2) the equation of Kelvin type:

$$P/P_s = \exp\left\{\frac{\gamma \cdot v_m}{RT} \cdot \frac{dA}{dV}\right\} \quad (3)$$

In particular, for cylindrical meniscus ( $n = 1$  in eq. (4)) or hemispherical one ( $n = 2$ )  $dA/dV$  is equal to  $n/(r_c - t)$ , where  $r_c$  is radius of cylindrical tube and  $t$  is adsorption film thickness. In this case well known "modified" Kelvin equation is obtained from eq. (3)

$$P/P_s = \exp\left\{\frac{n \cdot \gamma \cdot v_m}{RT \cdot (r_c - t)}\right\} \quad (4)$$

For the analysis of stability of different liquid-vapor configurations inside voids it is necessary to express the increment of interface area,  $dA$ , and that of volume,  $dV$ , in terms of multimolecular film thickness,  $t$ , and use the analytical expressions  $A = A(t)$  and  $V = V(t)$ , consisting of several components referred to near-neck toroidal configurations, menisci and spherical layers on cavities walls. Corresponding example for the cavity in Fig. 2 is presented in the Appendix for the case of de Boer - Linsen "universal isotherm" (in nm):

$$t = 0.354 [5/\ln(P_s/P)]^{1/3} \quad (5)$$

Now, having introduced into equation (3) for the critical relative pressure a certain multiplier accounting for interaction between the material adsorbed and solid surface, and at the same time, the intermolecular interaction of films on the opposite pore walls, we obtain:

$$P/P_s = M(P/P_s) \exp\left\{\frac{\gamma \cdot v_m}{RT} \cdot \frac{dA}{dV}\right\} \quad (6)$$

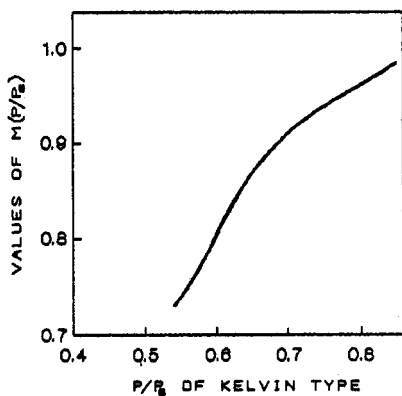


Fig. 3. Function  $M$  correcting Kelvin critical pressures.

The correction function,  $M$ , has been obtained as a result of processing the recent publications (refs. 3 - 10) on investigation the phenomenon of adsorption and capillary condensation by molecular physics techniques. We have performed our own calculations at the adsorption of model nitrogen in cylinders at  $T = 77.4$  K, basing on the local approximation of density functional theory. Parameters of nitrogen and molecules of solid surface were chosen exactly as in ref. 10. The details of these computations and the results of simulating the adsorption in the above voids with different numbers and sizes of necks by Monte - Carlo method will be published separately.

On comparison of data available and obtained it is established that for the temperatures distinctly lower than the critical one both in cases of cylinders and slits approximately the same disagreement between Kelvin and molecular physics critical relative vapor pressures is preserved (for not very small pores). It seems, this suggests that in case of the above-mentioned spheroidal voids with circular windows the analogous dependence will also satisfactorily correct the obtained results of Kelvin type. Fig.3 presents the averaged scheme of correction function for capillary condensation of nitrogen in case of local approximation of density functional theory.

It seems useful to make several predictions concerning the irreversible capillary condensation in the above voids that could be supposed to occur on the basis of analysis of rather a rough equation (3). With increasing the adsorbate vapor pressure the volume of material sorbed in the void will increase at approximately the same rate as in cylinder. However, as the quantitative estimation shows the general rate of decreasing the interface area will be retarded by the local

increase of the area near the necks. As a result, the delay in irreversible filling of the separate void (in relation to pressure increase) occurs, that must depend on the quantity of necks and the values of their radii. Hence it follows that the normal independent development of adsorption in a particular void of the system breaks down when in the neighboring void an irreversible capillary condensation has taken place. In fact, in this case in one of the necks a concave meniscus appears, which abruptly changes  $dA$  value. In other words, a definite small increase in area near the necks stepwise results in its considerable decrease. Moreover, the step being large enough, the premature spontaneous filling of the void considered is getting possible. In respect to the whole system of interrelated voids one can suppose that at the initial stage an evident phenomenon of delay in irreversible capillary condensation occurs. Then the "separate" filling of voids starts. As this takes place the situation in neighbouring cavities dramatically changes causing their cooperative filling associated with appearing of menisci in the necks. Obviously, the initial effect of the above "delay phenomenon" weakens. As the quantity of capillary condensate in the system increase, so does the possibility of sudden appearance of two and more menisci in the necks of free voids. This must result in increasing the portion of porous space elements filled according to cooperative mechanism. The possibility of this mechanism becoming dominating from the definite moment, should not be ruled out.

In closing of this section it should be noted in our numerical adsorption-desorption experiment we did not take into consideration the change in density of adsorbed layers and that of a condensate in filled voids. One can try to correct for the change of density either according to Steele (ref. 24), or in correspondence with ref. 10, or, what seems most reliable, based on the study of adsorbate and condensate density in the above voids by Grand Canonical Monte Carlo techniques or by molecular dynamics simulation.

### DESCRIPTION OF NUMERICAL EXPERIMENTS

At the initial stage of experiment until the spontaneous filling of at least one void was observed, each cavity in the lattice was analysed using the relationship (7) at each  $P/P_s$  only once. Then we carried out successive calculation of volumes of pseudoliquid configurations elements in each void (see Appendix) and their summing over the whole lattice. When at least even one void satisfied the unequality

$$P/P_s \leq M(P/P_s) \exp \left\{ \frac{\gamma \cdot v_m}{RT} \cdot \frac{dA}{dV} \right\}, \quad (7)$$

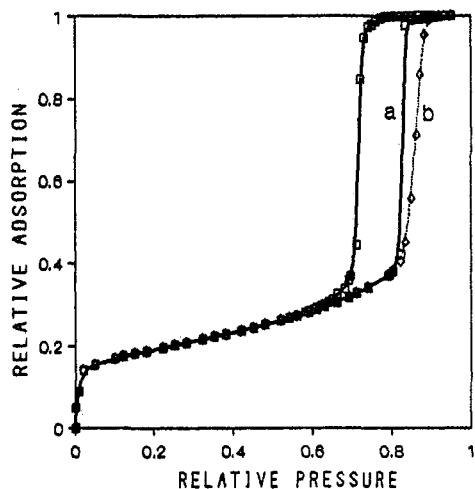


Fig. 4. Isotherms obtained from numerical adsorption experiments: a - filling of system of interrelated voids; b - filling of the same voids separated in space.

we performed a second analysis of situation in all the lattice voids situated next to the filled ones. Such a procedure was repeated at each  $P/P_s$  until at the next full analysis of the lattice the absence of new filled voids was observed. Only after that the volumes were calculated and summed to obtain the next experimental "circle" of model isotherm. To have a better idea about the effect of cooperative filling we have obtained one more isotherm supposing all the voids to be spatially separated. Using Fig. 4 one can compare an satellite isotherm (b) (dotted line) with the principal one (a) - (solid thick line) exhibiting a vastly more steep slope in the region of high filling of porous space with condensate.

To obtain the desorption branch of isotherm an algorithm of preliminary percolation sounding was used, described in detail in ref. 18. At the moment of beginning the desorption thickness of film in the necks was estimated basing on approach developed in refs. 16 and 25 but as applied to the curvature of toroidal surfaces. The value of critical meniscus was calculated as suggested by Nicholson (ref. 16) for circular cylindrical capillaries. We must admit that the adopted by us scheme of estimation the individual desorption of capillaries is not accurate enough but at present we do not have sufficient information (based for example on molecular physics approach) for more precise estimation of critical values of film thickness and meniscus in the similar configurations. For this reason in addition to the principal

adsorption experiment we performed an auxiliary experiment on mercury intrusion into the same porous solid.

As is known, percolation regularities of mercury intrusion are similar to those of vapor desorption (ref. 12). However, in case of mercury penetration the difficulties disappear, associated with estimation of critical values of multimolecular film and transverse radius of meniscus in the neck. At the mercury intrusion all geometrical configurations were estimated using Laplace law and the predetermined values of contact angle between mercury and solid surface ( $140^\circ$ ). The only uncertainty associated with arbitrary way of choosing the contact angle (in supposition that model porous solid is non-unshrinkable and its surface is not amalgamated) is of no importance in calculation the apparent volume or surface area PSD if one and the same value is used for producing the model program and in calculations following.

Computer experiment on random intersecting length distribution (RILD) calculation was carried out in a somewhat different way than those on adsorption or mercury intrusion. It was supposed that in the centre of single void, 5 nm in radius, the origin of Cartesian coordinates is situated so that each of three axes passes through the centers of two opposite necks (windows). For this void six neck radii were generated ( using a random-number generator ) in correspondence with PSD previously used for adsorption and mercury porosimetry. After that three random coordinates  $x_1, y_1, z_1$ , of the point lying inside the void were produced, and so were the three random cosines  $l, m, n$ , of any direction in three-dimensional space. Thus, we obtained the equation of a random straight line (RSL):

$$(x-x_1)/l = (y-y_1)/m = (z-z_1)/n \quad (8)$$

and started to look successively for the intersection of the RSL first with each of six windows inside the necks. For

instance, for the positive direction of abscissa it meant a simultaneous solution (8) and

$$x = (5^2 - r_{x+}^2)^{0.5}$$

$$y^2 + z^2 \leq r_{x+}^2$$

where  $r_{x+}$  is the radius of a corresponding neck. If RSL did not pass through two windows at a time we looked for the intersections with each of six toroidal patches of surface near the necks. For example, in case of positive direction of applicate axis, equation (8) was solved simultaneously with

$$[x^2 + y^2 + (z - z_0)^2 + r_{z+}^2 - \rho_0^2]^2 = 4 \cdot r_{z+}^2 \cdot (x^2 + y^2) \quad (9)$$

$$z_0 = (5^2 - r_{z+}^2)^{0.5}$$

where  $\rho_0$  - is the radius of neck toroidal chamfers. In this case coordinates of intersection points with tore  $x_1, y_1, z_1$ , (provided that (8) and (9) had at least one simultaneous solution) must have satisfied the following conditions

$$(x_1^2 + y_1^2) \leq r_{z+} - \rho_0 \cdot (r_{z+} + \rho_0) / (5 + \rho_0)$$

$$z_1 < z_0$$

(intersection point must lie inside the void). If in the first two cases two intersections (with windows and/or toroidal part of the surface) were not found, equation (8) was solved simultaneously with sphere equation:

$$x^2 + y^2 + z^2 = 5^2$$

Furthermore, if the straight line had two intersections with void surface, its length was calculated at once and to the corresponding element of RILD array 1 was added. If RSL "went out" through the window, this window was interfaced with an adjacent void 5 nm in radius. In other words, five more radii of necks were generated and the origin of Cartesian coordinates was transferred to the centre of new adjacent void. After that the procedure of search for intersections of (initial) random straight line with the surface of (new) void was repeated. This was continued until two intersections of a random straight line with the surface of solid phase were detected. The length of a random chord was calculated by summing up the segments belonging to the voids of chain obtained. Then a new "starting" void was generated and analysis of a new chain (that could consist of one void only) was performed. At the top of Fig. 7 one can see RILD obtained from the processing of 75000 chains with total number of voids more than 500000 (instead of the full length half-length of chords were plotted on the abscissa)

It should be noted, that PSD shown in Fig. 7 on the lower right was calculated basing on SPS model in accord with algorithm tested in ref. 26. Although the above numerical experiment does not accurately correspond to the procedure of processing the photomicrographs of porous samples sections, one can show as well as in ref. 27 that PSD obtained from RILD must be exactly the same as for the flat section of the porous solid. It is worth nothing that results of the last experiment might be of interest not only for realistic description of porous structure characteristics based on microscopy data but also in case of any physical technique employing ray or particle scattering in porous media.

## DISCUSSION

Before performing the comparative analysis of calculated (on the basis of isotherms, porogram and RILD) and initial PSDs it seems necessary to dwell on dissimilarity (from the point of view of physics) of distributions compared. In the case of neck radius distribution we deal with classical probability density,  $p(r)$ , i.e., the randomly chosen in lattice constriction belongs to radii interval,  $dr$ , with probability  $p(r)dr$ . In other cases instead of density plot  $p(r)$  considered are either density curves  $\pi r^2 Lp(r)$  (adsorption and mercury penetration), where  $L$  is a certain length of cylinders, or density curves  $(4\pi/3) r^3 p(r)$  (RILD). Evidently, in general case number and volume density functions must differ

considerably. However, due to fairly narrow neck size regions the obtained adsorption, mercury-porosimetry and desorption volume size distributions in respect to cylinders radii practically do not differ in the given scale from the corresponding distributions of number and surface area. In this connection, axes of ordinates and captions to them in Figs. 5 - 7 are omitted.

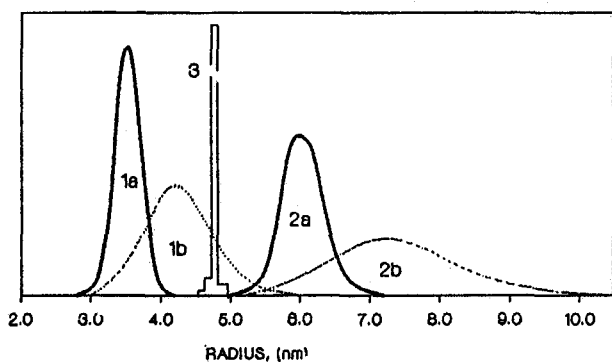


Fig. 5. Comparison of adsorption PSDs with the initial voids halfsize distribution: 1a - at the processing of the principal isotherm (curve a in Fig. 4)  $n = 1$  was used in eq. (4) (cylindrical meniscii); 1b - the same for an auxiliary isotherm (curve b in Fig. 4); 2a - when processing the principal isotherm hemispherical menisci (cylinders with bottom) were used; 2b - the same for an auxiliary isotherm; 3 - volume void distribution with respect to statistical halfsize.

A very narrow and high histogram near the marker 5 nm in Fig.5 represents the density function of distribution of void volume of model porous solid in respect to average semilengths of random chords passing through the centres of voids (i.e. through the centres of forming spheres). The other curves describe the densities of "adsorption" distributions of total pores volume normalized to unit area. Smooth curves (1a and 2a) are the densities of volume distribution in respect to radii of independent cylindrical capillaries, obtained at the processing of principal adsorption isotherm (a). In particular, curve 1a is calculated by Cranston and Inley method (ref. 15) interpreting the filling of cylindrical capillaries with the bottom. When calculating PSD for bottomless cylinder (curve 2a)

the same algorithm and the same analytical expression (5) for the thickness of multimolecular layer were used, though in numerator of Kelvin equation (4)  $n = 2$  was substituted for  $n = 1$  (cylindrical form of meniscus). Despite the fact that the model of independent cylinders with bottom must, seemingly, describe the process of filling the real porous solid more adequately, the average pore radius (6.0 nm) obtained according to Cranston - Inkley techniques differs from the "true" average void halfsize (4.8 nm) no less than the average radius of cylinders open on both ends (3.6 nm).

Detailed analysis of the reasons causing a discrepancy between the average radii values is too difficult. One can say with confidence, however, that one of the main reasons of such a discrepancy in case of cylinders with bottom is the above discussed phenomenon of delay in filling the voids which is due to presence of necks. In the second case, the discrepancy between average radii can be attributed both to the difference of critical liquid/vapor configuration forms in open cylinders and in the voids described, and to imperfection of Kelvin equation for the formal calculation of distributions.

The width of "apparent" PSDs is considerably more than the "true" one despite the phenomena of cooperative filling favorable for obtaining the more narrow distribution densities calculated formally. Fig. 5 illustrates the aforesaid more vividly, depicting distribution densities calculated for the auxiliary isotherm (b) (all the voids are separated in space). Now the ranges of model cylinders radii exceed by an order an interval of voids halfsizes. Although this case presents an interest only from theoretical point of view, it is worth noting that the average radius of cylinders with bottom differs approximately by 50% from the true one (in comparison with 25% for the main isotherm). Basing on the last observation one can suppose that Kelvin interpretation of spontaneous filling the through cylinders too rough for so little radii corresponds well to the delay in individual capillary condensation in voids of approximately the same size, having six necks of radius slightly more than that of the void.

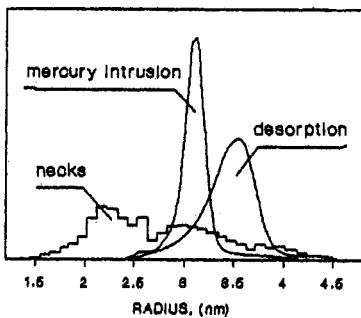


Fig. 6. Comparison of predetermined neck radius distribution with mercury - porosimetry and desorption distributions.

Histogram of number density function of "true" neck radius distribution (Fig. 6) is related to "differential" volume size distribution curves calculated from desorption branch of isotherm and model curve of mercury intrusion. The first thing that should be noted is a relatively satisfactory correspondence between mercury - porosimetry and desorption PSDs. Both the distributions are located in the region of the larger neck radii, though neither in shape nor in width they correspond to the true neck radius distribution. Basing on both capillary radius distributions calculated we should like to mention that a certain number of the largest necks and a considerable portion of the smallest ones are not covered. The first phenomenon can be easily explained basing on the concepts borrowed from percolation theory ( refs. 12, 13 and 28 ): for the global penetration of menisci inside porous space to begin, a sufficiently large portion of necks must accumulate, whose radii satisfy Kelvin (or Washburn for mercury (ref. 29)) condition. Thus, the largest necks of interrelated pore system practically do not inhibit the menisci after the beginning of global penetration, do not reveal themselves at the isotherm (mercury program) and, hence, can not appear in interpretation of desorption (mercury

intrusion) for model independent capillaries. The smallest necks in interrelated system (approximately the half of all the necks) are not reflected in calculated PSDs, since desorption (mercury) menisci penetrate inside the porous solid through relatively larger necks. In this connection it should be noted that location of narrow peaks of desorption or mercury-porosimetry PSD can change depending on average coordination number (connectivity) of porous space (refs. 12 and 13). In the above model porous solid each of the voids had 6 holes. It is evident that elimination of a considerable portion of necks in the lattice will result in decrease of menisci penetrability. The latter will manifest itself in corresponding shift of mercury program or desorption isotherm to the left, and, hence, in the shift of formally calculated PSDs in direction of smaller radii. At the same time, there is good reason to believe that distribution width must not significantly depend on the change of average number of necks per each void (ref. 12 and 13).

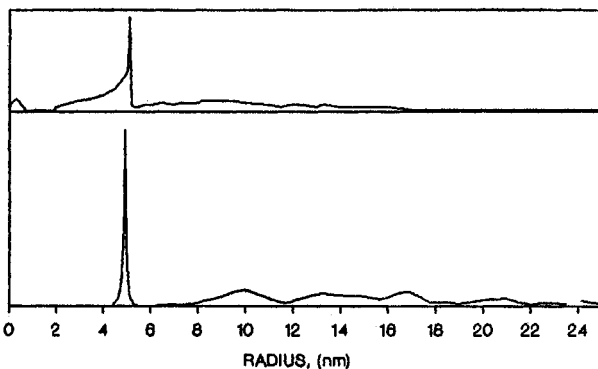


Fig. 7. At the top: random intersecting (half)length distribution (RILD) in above model porous space; at the bottom: PSD calculated from RILD using sphere pore segment (SPS) model.

In respect to the PSD obtained in ref. 1 from mercury intrusion data (Fig. 1) one can say with confidence that as well as in the above case it is far from covering the whole range of constriction sizes in porous space of material studied. Probably, the difference between typical sizes of constrictions and widenings in real porous systems is not so large as one can think analyzing Dullien et al works. There is one more ground in favour of this conclusion: during the scanning of contrast photomicrographs of porous solid cuts the ray of scanner must, from time to time, continuously pass through two or several connected voids of structure. At the interpretation based on SPS model this will be considered as presence of very large cavities. Hence, the possibility of "photomicroscopic" distribution (Fig. 1) containing at the right rather a long and thick fictitious part should not be ruled out.

The aforesaid is completely confirmed by results of processing the RILD using SPS model. Figure 7, bottom, depicts the calculated PSD, consisting of

separate sharp peak near mark 5 nm and long wavy curve in region of large radii. The peak on mark 5 nm corresponds to the radius of model porous solid voids for which RILD was calculated, and fits the case when the chains in the above experiment consisted of one cavity only. However, the area of this peak constitutes a mere 11-12% from the total area under distribution curve. The remainder "fictitious" part of area correspond to the case when the chains of voids strung on random chords consisted of two and more voids. At the further processing of RILD obtained using SPS model these long random chords were considered as belonging to separate large spheres.

## CONCLUSIONS

Basing on the investigations performed in this work, one can draw the following conclusions:

**In respect to adsorption:** shape and width of adsorption branch of experimental isotherms are affected on the one hand by the average number of necks per void (that influences the degree of delay and development of capillary condensation in the system of interrelated mesopores), and on the other hand by the effect of cooperative filling the voids with condensate at the later stage of adsorption. None of the known methods of calculating the PSDs does not take these two things into consideration, including a recently developed method (ref. 10) based on molecular physical concepts. Because of this, shape and width of distributions calculated formally on the basis of adsorption branches of real isotherms can substantially differ from the true PSDs. The average diameters of cylindrical capillaries assumed in calculations are the highest (cylinders with bottom) and lowest (bottomless cylinders) estimations of the average characteristic size of widenings of porous space. It is not improbable that the true characteristic size is closer to the average value of model bottomless cylinders.

**In respect to desorption and mercury porosimetry:** interrelation of mesopores is responsible for the initial delay in global penetration of menisci inside the porous solid. However, percolation threshold being achieved, the accelerating process of freeing from condensate (filling with mercury) proceeds through the necks of middle sizes. Considerable portion of the smallest necks "do not have a chance to come into action". Therefore, the width of formally calculated PSD appears to be sufficiently smaller than in reality. The shape of calculated distributions as well as in case of adsorption branch, is a result of complex real process in the system of interrelated mesopores and does not reflect the true constriction size distributions. However, size ranges obtained at the formal processing of desorption isotherms and mercury intrusion curves (porograms) lie most probably within the limits of real intervals of neck sizes. Desorption and mercury-porosimetry average radii of capillaries are the result of approximate estimation of the average radius of mesoporous space narrowings which depends on the average number of necks per void in the system.

Finally, the difference between the sizes of narrowings and broadenings in real mesoporous materials is not so great as one can think when correlating the results of interpretation of mercury porosimetry data and statistical processing of photomicrographs. Excessive difference is due to imperfection of the model of independent capillaries (mercury porosimetry) and the model of independent spherical segments.

## APPENDIX

When calculating the components of volume and surface area of material sorbed, as an independent variable one can take the thickness of multimolecular layer,  $t$ , (connected with the relative vapor pressure by eq. (5) of the principal part of text). Obviously, equilibrated radius of menisci in the necks is expressed in terms of eq. (5) and Kelvin equation (4) as

$$R_k = (\gamma \cdot v_m \cdot n \cdot t^3) / \{5RT (0.354)^3\} \quad (A1)$$

Angles  $\alpha_1$  and  $\alpha_2$  in Fig. 2 are equal to

$$\alpha_1 = \arccos \{(r_1 + \rho_0) / r_p\} \quad (A2)$$

where the neck radii,  $r_i$  ( $i=1,2$ ), void radius,  $r_0$ , and the radius of neck toroidal chamfers,  $\rho_0$ , are assumed on generating the model porous space.

Volume,  $V_{is}(\alpha_1, r + \rho_0, t + \rho_0)$ , and surface area,  $A_{is}(\alpha_1, r_1 + \rho_0, t + \rho_0)$  of toroidal sector (sections ABC and DEF in Fig. 2) are expressed by formulae "hard-to-get-at" in reference literature but quite simple and accurate

$$V_{is}(\alpha_1, r_1 + \rho_0, t + \rho_0) = \pi \cdot (t + \rho_0)^2 \cdot \{\alpha_1 \cdot (r_1 + \rho_0) - (2/3) \cdot (t + \rho_0) \sin \alpha_1\} \quad (A3)$$

$$A_o = A_{is}(\alpha_1, r_1 + \rho_0, t + \rho_0) = 2\pi \cdot (t + \rho_0) \{\alpha_1 \cdot (r_1 + \rho_0) - (t + \rho_0) \sin \alpha_1\} \quad (A4)$$

Where sector angle,  $\alpha_1$ , is measured in radians from horizontal. Ring-like volume of liquid in the lower neck is equal to

$$V_o = V_{is}(\alpha_1, r_1 + \rho_0, t + \rho_0) - V_{is}(\alpha_1, r_1 + \rho_0, \rho_0) \quad (A5)$$

Angle  $\beta = \beta(t)$  (neck on the right) is determined by the radii of the void,  $r_p$ , of the neck,  $r_2$ , and of neck chamfer,  $\rho_0$ , as well as by the thickness of multimolecular layer,  $t$ :

$$\beta(t) = \arccos \{(r_2 + \rho_0) / (R_k(t) + t + \rho_0)\} \quad (A6)$$

The volume of narrow ring of adsorbate (sections GHIJ and KLMN) is equal to

$$V_1 = \{V_{\text{is}}(\alpha_2, r_2 + \rho_0, \rho_0 + t) - V_{\text{is}}(\alpha_2, r_2 + \rho_0, \rho_0)\} - \{V_{\text{is}}(\beta, r_2 + \rho_0, \rho_0 + t) - V_{\text{is}}(\beta, r_2 + \rho_0, \rho_0)\} \quad (\text{A7})$$

and its surface area is

$$A_1 = A_{\text{is}}(\alpha_2, r_2 + \rho_0, t + \rho_0) - A_{\text{is}}(\beta, r_2 + \rho_0, t + \rho_0) \quad (\text{A8})$$

The remainder volume of liquid inside the cone OPQ is

$$V_2 + V_{\text{con}} - V_{\text{ss}} - V_{\text{is}2} \quad (\text{A9})$$

where expressions for volume of cone with section SPQ,  $V_{\text{con}}(\beta, r_2 + \rho_0)$  and the volume of spherical sector with section SJK,  $V_{\text{ss}}(\beta, R_k)$  can be found in any handbook of mathematics (see, for instance ref. 30).  $V_{\text{is}2}(\beta, r_2 + \rho_0, \rho_0)$  is the volume of toroidal sector with sections PIU and VLQ.

The area of liquid/vapor interface in cone SPQ corresponds to the area of spherical sector SJK (meniscus)

$$A_2 = 2\pi R_k^2 \cdot (1 - \sin \beta) \quad (\text{A10})$$

The total volume of "liquid" inside the cavity is expressed as

$$V(t) = (4\pi/3) \{r_p^3 - (r_p - t)^3\} + V_0 + V_1 + V_2 - V_3 - V_4 \quad (\text{A11})$$

where  $V_3$  is the difference of volumes of spherical sectors with sections HOM and GON,  $V_4$  is an analogous difference of volumes for the lower neck.

The area of liquid surface inside the cavity in Fig. 2 is equal to

$$A(t) = 4\pi(r_p - t)^2 + A_0 + A_1 + A_2 - A_3 - A_4 \quad (\text{A12})$$

where  $A_3$  is the area of spherical sector GON,  $A_4$  is the area of a similar sector for the lower neck (BOE).

Expressions (A1) - (A12) can be easily differentiated with respect to  $t$  using derivative tables and the rules of differentiation of composite functions, in order to find the analytical expressions for  $dA/dt$  and  $dV/dt$ , used in relationship (3) and (6) in the principal part of the text.

## REFERENCES

1. F.A.L. Dullien and G.K. Dhawan, *J. Colloid Interface Sci.*, **47**, 337 (1974).
2. S.J. Greg and K.S.W. Sing, *Adsorption, surface area and porosity*, Academic Press, London (1982).
3. G.S. Heffelfinger, Fr. van Swol, K.E. Gubbins, *Molec. Phys.*, **61**, 1381 (1987).; Fr. van Swol and K.E. Gubbins, in *T. International Symposium on Thermodynamics in Chemical Engineering and Industry*, Ithaca, NY (1988).
4. B.K. Peterson and K.E. Gubbins K.E., *Molec. Phys.*, **62**, 215 (1987).
5. B.K. Peterson, Gubbins K.E., Heffelfinger G.S., U. Marini Bettolo Marconi and Fr. van Swol, in *School of Chemical Engineering*, Cornell University, Ithaca, NY (1988).
6. R. Evans, U. Marini Bettolo Marconi, H.H. Wills, P. Tarazona, *J. Chem. Soc. Faraday Trans. 2.*, **82**, 1763 (1986).
7. P. Tarazona, U. Marini Bettolo Marconi, R. Evans, *Molec. Phys.*, **60**, 573 (1987).
8. Z. Tan and K.E. Gubbins, in *Characterization of Porous Solids II*, p. 21, Elsevier, Amst. (1991).
9. B.K. Peterson, K.E. Gubbins, G.S. Heffelfinger, U. Marini Bettolo Marconi and Fr. van Swol, *J. Chem. Phys.*, **88**, 6487 (1988).
10. N.A. Seaton, J.P.R.B. Walton and N. Quirke, *Carbon*, **27**, 853 (1989).
11. J.C.P. Broekhoff and J.H. De Boer, *J. Catalysis*, **9**, 8 (1967).
12. G.C. Wall and R.J.C. Brown, *J. Colloid Interface Sci.*, **82**, 141 (1981).
13. V.P. Zhdanov, V.B. Fenelonov and D.K. Efremov, *J. Colloid Interface Sci.*, **120**, 218 (1987).
14. S.R. Broadbent and J.M. Hammersley, *Proc. Camb. Phil. Soc.*, **53**, 629 (1957).
15. R.W. Cranston and F.A. Inkley, *Advan. Catalysis*, **9**, 143 (1957).
16. D. Nicholson, *Trans. Faraday Soc. II*, **64**, 3416 (1968).
17. I.E. Melrous, *Canad. J. Chem. Eng.*, **48**, 638 (1970).
18. D.K. Efremov and V.B. Fenelonov, in *Characterization of Porous Solids II*, p. 115, Elsevier, Amst. (1991).
19. D.K. Efremov and V.B. Fenelonov, in *7th International Symposium on Theoretical Adsorption*, p. 111, Nauka, Moscow (1991), (in Russian).
20. J.C.P. Broekhoff and J.H. De Boer, *J. Catalysis*, **10**, 153 (1968).
21. M.M. Dubinin, L.I. Kataeva and V.I. Ulin, *Izv. AN USSR, ser. chem.*, No. 3, 510 (1977), (in Russian).
22. L.H. Cohan, *J. Am. Chem. Soc.*, **60**, 433 (1938).
23. J.F. Gibbs, in *Scientific Papers*, p. 43, Longmans, NY (1928).
24. W.A. Steele, *J. Colloid Interface Sci.*, **75** (1980).
25. J.H. De Boer, B.G. Linsen, J.C.P. Broekhoff and Th.J. Osinga, *J. Catalysis*, **11**, 46 (1968).
26. A.G. Spector, *Zavod. Lab.*, **16**, 173 (1950).
27. F.A.L. Dullien, E. Rhodes and S. Schrocter, *Powder Technol.*, **3**, 124 (1969/70).
28. L.I. Kheifets and A.V. Neimark, *Multiphase Processes in Porous Media*, Khimia, Moscow (1982), (in Russian).
29. E.W. Washburn, *Proc. Nat. Acad. Sci. U.S.A.*, **7**, 115 (1921).
30. I.N. Bronstain and K.A. Semidjajev, *Mathematical Handbook*, p. 189, Nauka, Moscow (1986), (in Russian).